J Antimicrob Chemother 2017; **72**: 727–734
doi:10.1093/jac/dkw514 Advance Access publication 20 December 2016

Journal of Antimicrobial Chemotherapy

Purification of Zika virus RNA-dependent RNA polymerase and its use to identify small-molecule Zika inhibitors

Hong-Tao Xu[1], Said A. Hassounah[1], Susan P. Colby-Germinario[1], Maureen Oliveira[1], Clare Fogarty[1], Yudong Quan[1], Yingshan Han[1], Olga Golubkov[1], Ilinca Ibanescu[1], Bluma Brenner[1], Brent R. Stranix[2] and Mark A. Wainberg[1,3,4]*

[1]*Jewish General Hospital, McGill University AIDS Centre, Lady Davis Institute for Medical Research, Montreal, Quebec, Canada;* [2]*Champlain Exploration Pharma Inc., Montreal, Quebec, Canada;* [3]*Department of Medicine, McGill University, Montreal, Quebec, Canada;* [4]*Department of Microbiology and Immunology, McGill University, Montreal, Quebec, Canada*

*Corresponding author. McGill University AIDS Centre, Lady Davis Institute for Medical Research, Jewish General Hospital, 3755 Côte-Ste-Catherine Rd, Montreal, Quebec, H3T 1E2, Canada. Tel: +1-514-340-8260; Fax: +1-514-340-7537; E-mail: mark.wainberg@mcgill.ca

Received 27 September 2016; returned 26 October 2016; revised 31 October 2016; accepted 1 November 2016

Background: The viral RNA-dependent RNA polymerase (RdRp) enzymes of the *Flaviviridae* family are essential for viral replication and are logically important targets for development of antiviral therapeutic agents. Zika virus (ZIKV) is a rapidly re-emerging human pathogen for which no vaccine or antiviral agent is currently available.

Methods: To facilitate development of ZIKV RdRp inhibitors, we have established an RdRp assay using purified recombinant ZIKV NS5 polymerase.

Results: We have shown that both the hepatitis C virus (HCV) nucleoside inhibitor sofosbuvir triphosphate and a pyridoxine-derived non-nucleoside small-molecule inhibitor, DMB213, can act against ZIKV RdRp activity at IC_{50}s of 7.3 and 5.2 μM, respectively, in RNA synthesis reactions catalysed by recombinant ZIKV NS5 polymerase. Cell-based assays confirmed the anti-ZIKV activity of sofosbuvir and DMB213 with 50% effective concentrations (EC_{50}s) of 8.3 and 4.6 μM, respectively. Control studies showed that DMB213 did not inhibit recombinant HIV-1 reverse transcriptase and showed only very weak inhibition of HIV-1 integrase strand-transfer activity. The S604T substitution in motif B of the ZIKV RdRp, which corresponds to the S282T substitution in motif B of HCV RdRp, which confers resistance to nucleotide inhibitors, also conferred resistance to sofosbuvir triphosphate, but not to DMB213. Enzyme assays showed that DMB213 appears to be competitive with natural nucleoside triphosphate (NTP) substrates.

Conclusions: Recombinant ZIKV RdRp assays can be useful tools for the screening of both nucleos(t)ide compounds and non-nucleotide metal ion-chelating agents that interfere with ZIKV replication.

Introduction

Zika virus (ZIKV) belongs to the family *Flaviviridae*, a group of enveloped positive-sense single-stranded RNA viruses and is transmitted by mosquitos, primarily the daytime-active female *Aedes aegypti*.[1,2] Although ZIKV was first isolated from a sentinel rhesus monkey placed in the Zika Forest near Lake Victoria in Uganda in 1947,[3] outbreaks of ZIKV have been reported since 2007 on Yap Island, the Federated States of Micronesia, and in 2013 in New Caledonia, the Cook Islands, French Polynesia and Easter Island.[4–6] Most recently, a widespread Zika epidemic has spread from Brazil to other parts of South and North America.[6,7] In February 2016, the WHO declared Zika to be a Public Health Emergency of International Concern (PHEIC).[8,9]

It is estimated that 80% of ZIKV infections are asymptomatic.[10,11] Recent studies have shown significant cellular death of neural stem cells once infected with ZIKV and animal models have demonstrated that ZIKV infection can lead to microcephaly in mice,[12,13] making clear that ZIKV is an emergent neuropathological agent.[14] Currently, there is no effective antiviral treatment for any flavivirus, including ZIKV and dengue virus (DENV), and no vaccine is available for either West Nile virus (WNV) or ZIKV.

ZIKV is a small enveloped virus, similar to other flavivirus structures,[15,16] and possesses a single-stranded positive-sense RNA genome of ∼11 kb, which encodes a single polyprotein flanked by 5′ and 3′ untranslated regions (UTRs).[17–19] This polyprotein of ∼3400 amino acids undergoes proteolytic cleavage by viral serine and cellular furin proteases to generate the capsid (C) protein, the precursor of the membrane protein (prM), and the envelope protein (E), as well as seven non-structural proteins (NS1, NS2A, NS2B, NS3, NS4A, NS4B and NS5).[18,19] The NS5 protein is ∼900 amino

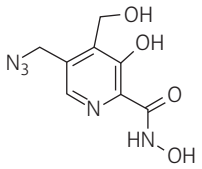

Figure 1. Structure of the non-nucleoside compound DMB213.

acids long and includes a methyltransferase domain at its N terminus and an RNA-dependent RNA polymerase (RdRp) domain at the C terminus.[1] Viral RdRps are essential for viral replication and are a significant target for development of direct-acting antiviral (DAA) agents, such as those that target the NS5B of hepatitis C virus (HCV), and, indeed, both nucleos(t)ide inhibitors (NIs) and non-nucleoside inhibitors (NNIs) have been approved for treatment of HCV infections.[20–22]

NS5 is the most conserved flavivirus protein, and several crystal structures of flavivirus NS5 and/or the polymerase domain have been solved.[23–28] Sequence analysis of the NS5 polymerase gene of ZIKV (data not shown) has revealed a high degree of homology with six conserved RdRp motifs of other flaviviruses, termed A–F, which play key roles in binding of each of RNA, nucleoside triphosphate (NTP) and metal ions as well as in catalysis.[28] The amino acids in the catalytic site of ZIKV RdRp are located within motif A (D536) and a catalytic GDD triad at position 665–667 (D666, D667) in motif C. The two latter aspartate residues are involved in the coordination of two divalent metal ion cofactors that are essential to the catalytic process, i.e. the 'two-metal-ion mechanism'.[29]

Viral RdRp inhibitors approved for the clinic include NIs that function as chain terminators of nascent nucleic acid production and NNIs. The NIs require intracellular phosphorylation by cellular kinases to a 5′-triphosphate form, following which they bind at the enzyme's active site and compete with natural substrates for incorporation.[30–32] By contrast, NNIs do not require intracellular activation and interfere with the chemical step of RNA synthesis by binding to allosteric sites remote from the active site of the RdRp.[32–35] NIs have been shown to be effective against HCV,[32] DENV,[33] tick-borne encephalitis virus (TBEV),[36] WNV[37] and yellow fever virus (YFV).[38]

Sofosbuvir was the first anti-HCV NI to be approved by the FDA in December 2013 and has a high genetic barrier to resistance as well as an excellent safety profile.[32] It is phosphorylated intracellularly to 2′-C-methyl-2′-fluoro-UTP.

Viral RdRps employ a mechanism for nucleotidyl transfer that involves two metal ions at the active site.[39] Metal-chelating agents represent an important NNI class of enzyme inhibitors[29–33] and chelation of the divalent metal ion cofactors of HIV integrase has led to the design and approval of raltegravir, elvitegravir and dolutegravir.[31] Metal chelation has also been effective in regard to inhibition of HCV polymerase[34,35] and influenza PA endonuclease 33 and the RdRp of DENV.[40]

In this study, we describe the expression, purification and characterization of ZIKV RdRp. We show that sofosbuvir triphosphate and a pyridoxine-derived small-molecule inhibitor, DMB213, can efficiently inhibit ZIKV RdRp activity in filter-binding enzyme assays and have verified these results in cell-based assays. Furthermore, we show that an S604T substitution in the ZIKV RdRp, corresponding to S600T in DENV RdRp and S282T in HCV RdRp, both of which were shown to be resistant to NIs,[30,32,41,42] conferred resistance to sofosbuvir, but not to DMB213. Thus, we have established novel RdRp assays for screening inhibitors that target ZIKV NS5 polymerase and have shown that both NI and NNI strategies could potentially be pursued as part of anti-ZIKV drug development.

Materials and methods

Compounds and nucleic acids

All DNA and RNA oligonucleotides used were purchased from Integrated DNA Technologies (IDT DNA, Coralville, IA, USA). Poly(rC) RNA and poly(rA)/oligo(dT)$_{12–18}$ were obtained from Midland Certified Reagent Company (Midland, TX, USA).

The ZIKV mini-genome (ZMG) consists of the first 228 nt of the 5′ end of genomic RNA plus three guanines and the last 533 nt at the 3′ end. ZMG DNA was derived by use of three PCR reactions that targeted the 5′ and 3′ ends of cDNA fragments that were reverse transcribed from ZIKV genome RNA (GenBank accession number KF993678, strain PLCal_ZV), using procedures employed for construction of the DENV mini-genome.[43] The first PCR was performed using the ZIKV 5′ end the cDNA fragment and employed forward primer ZVOPT7F [5′-TAATACGACTCACTATAGGGAGTTGTTGATCTGTGTG-3′ (the T7 promoter and the three extra guanines are underlined)] and the reverse primer ZVOPR1 [5′-ATCACCTATGATCCTGCGCACCATGTTGACCCAGCAGAAGTCCGGC-3′ (the overlapped region with the 5′ end of the product from the second PCR is underlined)]. The second PCR was performed using the ZIKV 3′-end cDNA fragment and primers ZVMGF2 (5′-AACATGGTGCGCAGGATC-3′) and ZV3′UTRR (5′-AGACCCATGGATTTCCCCACACCGGCCG-3′). The PCR products of PCRs 1 and 2 were purified through 1% agarose gel electrophoresis, annealed and then used as PCR templates using primers ZVOPT7F and ZV3′UTRR. The DNA product was purified through 1% agarose gel electrophoresis and used as a DNA template for *in vitro* transcription to produce a 764 nt RNA template containing the 3′ end of genomic ZIKV RNA and three extra guanines upstream of its 5′ terminus, using an Ambion T7-MEGAscript kit (Thermo Fisher Scientific Inc., Mississauga, ON, Canada) (using protocols provided by the manufacturer).

Sofosbuvir and its active form, sofosbuvir triphosphate, were obtained from Gilead Sciences Inc. 3′-dGTP was obtained from TriLink BioTechnologies (San Diego, CA, USA). Mycophenolic acid was obtained from Sigma-Aldrich (Markham, ON, Canada).

Preparation of DMB213

DMB213 (Figure 1) was identified by screening a small library of pyridoxine-derived small-molecule compounds[44] that were constructed through drug-design protocols aimed at chelating the divalent metal ions from the catalytic sites of viral enzymes such as HIV integrase and DENV RdRp.[40,44]

Construction of ZIKV NS5 polymerase bacterial expression plasmids and expression of Zika NS5 polymerase

The gene encoding the ZIKV NS5 polymerase domain was synthesized via GeneArt Gene Synthesis (Thermo Fisher Scientific Inc.), based on the ZIKV genome sequence (GenBank accession number KU321639.1).[45] BspHI and XhoI were used to digest the 5′ and 3′ ends, respectively, and after digestion with BspHI and XhoI, the fragment was cloned into the NcoI and XhoI sites of pET28b vector (Novagen). The final construct (pET28bZVNS5PolcHis6) was confirmed by sequencing and used for expression and purification of the recombinant ZIKV RNA polymerase domain containing a carboxyl-terminus hexahistidine tag in *Escherichia coli*. The amino acid substitutions S604T in motif B and mGDD (containing the D666A/D667A double mutations) in motif C were introduced into ZIKV virus NS5 polymerase using the Quick-change mutagenesis kit (Agilent Technologies Canada Inc., Mississauga, ON, Canada)

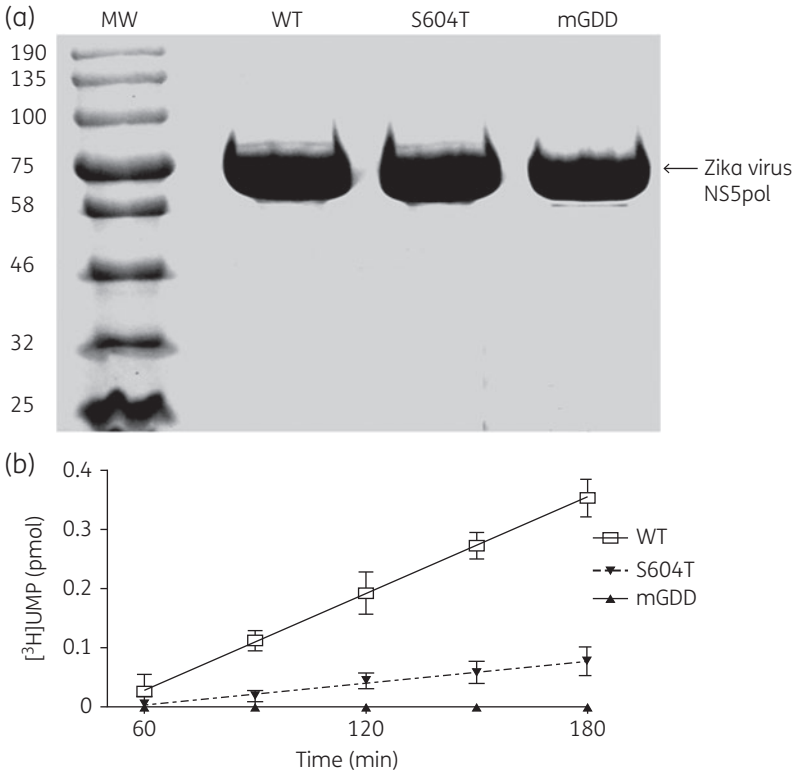

Figure 2. Purification and activity of ZIKV recombinant NS5 polymerase domain WT (ZIKV NS5pol) and mutants. (a) Coomassie brilliant blue staining of purified NS5 polymerase domains after 10% SDS–PAGE. MW, molecular size standards in kDa. The positions of purified recombinant NS5 polymerase domains are indicated on the right. The mutant mGDD contains the active site substitutions GDD to GAA. (b) Activity of recombinant ZIKV NS5 polymerase domains as assessed using ZMG RNA template by filter-binding RdRp assay as described in the Materials and methods section. Values are the means of two independent experiments. Error bars represent standard deviations.

and pET28bZVNS5PolcHis6 DNA as template. The highly conserved motif B of RdRp in ZIKV NS5 'Q_{601}R**S$_{604}$**GQVVTYALNTF$_{615}$' is identical to those of WNV and Japanese encephalitis virus.[27,46] Expression and purification of recombinant Zika NS5 polymerase were as recently described for the polymerase of DENV.[46]

Establishment of a de novo RdRp assay using recombinant ZIKV NS5 polymerase and heteropolymeric ZIKV mini-genomic RNA

Flaviviridae RdRp enzymes carry out RNA synthesis through a *de novo* initiation mechanism.[2,47] We evaluated the ZIKV NS5 polymerase in reactions employing ZMG RNA as template in order to screen NIs and NNIs. Optimal reaction conditions were similar to those previously described for the RdRp of DENV.[46]

Establishment of a primer-dependent RdRp assay using recombinant ZIKV NS5 polymerase and homopolymeric RNA

Flaviviridae RdRp enzymes can efficiently use homopolymeric RNA template as an efficient substrate.[46,48] Therefore, we established a ZIKV primer-dependent RdRp filter-binding assay that employed homopolymeric poly (rC) RNA template/rG_{13} primer (T/P) as a screen for NNIs. We began with procedures used for DENV RdRp,[46] which were optimized for ZIKV NS5 polymerase. A 20 μM T/P stock solution was prepared by annealing the RNA primer rG_{13} to poly(rC) RNA template at an equal molar ratio in a buffer containing 50 mM Tris (pH 8.0) and 50 mM NaCl by heating at 95 °C for 5 min, then slowly cooling to room temperature using a heat block. The RdRp reaction mixture contained 20 mM Tris–HCl (pH 6.8), 10 mM NaCl, 0.5 mM TCEP [Tris(2-carboxyethyl)phosphine], 0.001% Igepal-CA630, 5% glycerol, 1 U/μL SUPERase In RNase Inhibitor (Thermo Fisher Scientific Inc.), 0.5 μM T/P poly(rC)/rG_{13}, 2.5 mM $MnCl_2$, 2.5 μM [^{3}H]GTP (~15 Ci/mmol, Perkin Elmer, Waltham, MA, USA) and recombinant enzyme in a final volume of 20 μL. The RdRp reactions were initiated by adding [^{3}H]GTP and incubation was maintained for 45 min at 30 °C, followed by addition of ice-cold 10% cold trichloroacetic acid (TCA) and 20 mM sodium pyrophosphate, following which the samples were kept on ice for at least 30 min. The precipitated products were processed as described above for the *de novo* RdRp assay. Calculations of IC_{50} values were as described above.

Evaluation of compounds against ZIKV replication in cell culture

ZIKV (strain PLCal_ZV) and Huh7 cells (kindly provided by Drs David Safronetz and Gary Kobinger, National Microbiology Laboratory of Canada) were used in our cell-based assays. Huh7 cells were maintained in 10% DMEM supplemented with 4 mM glutamine, 100 U/mL penicillin and 100 mg/mL streptomycin. The $TCID_{50}$ of ZIKV was determined by the Promega Viral ToxGlo Assay (Fisher Scientific, Ottawa, ON, Canada) in Huh7 cells. Cell-based assays for evaluation of antiviral activity against ZIKV were performed using the Viral ToxGlo Assay (Fisher Scientific, Ottawa, ON) following the manufacturer's instructions.

Table 1. Inhibition of ZIKV polymerase activity by sofosbuvir triphosphate in a *de novo* RdRp assay

	IC_{50} (μM)[a]	
	WT	S604T[b]
Sofosbuvir triphosphate	7.3 ± 0.9	36 ± 3.7
3′-dGTP	0.7 ± 0.2	0.8 ± 0.3

[a]Determined by *in vitro* filter binding *de novo* RdRp assay at 30 °C for 120 min using purified ZIKV NS5 polymerase domains and ZMG RNA template at 500 μM each of ATP, CTP, GTP (or 5 μM GTP for 3′-dGTP) and 5 μM [^{3}H]UTP. Data represent the means ± SD of three independent experiments.
[b]The S604T substitution was introduced into the ZIKV NS5 polymerase domain by site-directed mutagenesis.

Table 2. Inhibition of ZIKV polymerase activity by the non-nucleoside DMB213 in a primer-dependent RdRp assay

	IC_{50} (μM)[a]	
	WT	S604T
DMB213	5.2 ± 0.9	4.2 ± 0.7
3′-dGTP	0.9 ± 0.2	0.9±0.3

[a]Determined by *in vitro* filter binding primer-dependent RdRp assay on a homopolymeric poly(rC)/rG13 substrate at 30 °C for 45 min using purified ZIKV NS5 polymerase domains and ZMG RNA template at 500 μM each of ATP, CTP, GTP (or 5 μM GTP for 3′-dGTP) and 5 μM [^{3}H]UTP. Data represent the means ± SD of three independent experiments.

Evaluation of DMB213 against HIV-1 reverse transcriptase (RT) and integrase activities

Subtype B HIV-1 WT RT and that containing the M184V substitution were generated as described previously.[49,50] A test of the inhibitory effect of DMB213 on HIV-1 RT activity was performed as described.[51] Recombinant subtype B HIV-1 integrase was expressed in and purified from *E. coli* BL21(DE3) cells as previously published.[52,53] Using the strand-transfer assay, the susceptibility of HIV recombinant integrase to DMB213 and integrase strand-transfer inhibitors (INSTIs) was assessed in the presence of DMB213 or INSTIs, including dolutegravir, elvitegravir and raltegravir.[52,53]

Molecular modelling

A homology model of Zika polymerase was generated using the I-TASSER protein structure prediction server.[54–56] Previously published structures were obtained through the Research Collaboratory for Structural Bioinformatics (RCSB) Protein Data Bank (http://www.rcsb.org/pdb/). Molecular modelling was performed using the published lead template of DENV NS5 RdRp (PDB ID: 2J7U).[25] The published structure of HCV NS5B in complex with Mn^{2+} and primer template (PDB ID: 4WTA) was also used for the generation of the Zika polymerase homology model.[57] The structure of DMB213 was generated from PubChem Sketcher V2.4 (http://pubchem.ncbi.nlm.nih.gov/edit) and used as a ligand. Minimization of ligand-docked structures was facilitated by the use of a UCSF Chimera (http://www.cgl.ucsf.edu/chimera/),[58] which prepared Zika polymerase and DMB213 as inputs for DOCK calculations, which predict the orientation of the ligand. Docking calculations were performed using AutoDock Vina,[59] The putative positions of Mg^{2+} and RNA were superimposed from published structures, i.e. 2J7U and 4WTA, respectively. The homology model was verified by Ramachandran plot analysis to have >97.6% of residues in allowed and favourable orientations.[60,61]

Table 3. Antiviral activity of various compounds against ZIKV

	EC_{50} (μM)[a]	CC_{50} (μM)[b]	SI[c]
Sofosbuvir	8.3 ± 1.6	>100	>12
DMB213	4.6 ± 1.0	22 ± 3.0	4.8
Mycophenolic acid	0.8 ± 0.3	>100	>100

[a]Determined in Huh7 cells using the Promega Viral ToxGlo Assay. Data represent the means ± SD of three independent experiments.
[b]Determined in BHK-21 cells using the Promega Viral ToxGlo Assay.
[c]Ratio of CC_{50} to EC_{50}.

Table 4. Influence of NTP concentration on the inhibitory activity of DMB213 on ZIKV NS5 polymerase activity[a]

GTP (μM)	DMB213 IC_{50} (μM)
1.5	3.8 ± 0.4
3	4.7 ± 0.9
15	20.1 ± 3.1
30	35.2 ± 4.7

[a]The effect of NTP concentration on the inhibitory potency of DMB213 was evaluated by filter-binding RdRp assay in the presence of various concentrations of [^{3}H]GTP and DMB213. Data represent the means ± SD of three independent experiments.

Results

Purification and characterization of ZIKV RdRp

Recombinant ZIKV NS5 WT polymerase and RdRp enzymes containing either an S604T substitution and or an mGAA (from mGDD) substitution in the active site were purified to >95% homogeneity under native conditions, as demonstrated by SDS–PAGE (Figure 2a). For characterization of enzyme activity, the rate of RNA synthesis was analysed by following the incorporation of radiolabelled nucleotide into newly synthesized RNA, which was separated from free radiolabelled nucleotide by TCA precipitation and filtration. Time course experiments were initiated by mixing together 400 nM purified NS5 polymerase with 100 nM RNA in RdRp assay buffer, thus, providing a means of comparing different NS5 polymerases (Figure 2b).

First, we observed that the S604T substitution caused a diminution in enzyme activity compared with WT, similar to results obtained with the S600T mutation in the DENV NS5 polymerase. The active-site RdRp mutant mGDD was completely devoid of enzyme activity. Thus, we confirmed that ZIKV RdRp activity is associated with the purified NS5 polymerase domain and that the active site GDD motif is essential for this activity.

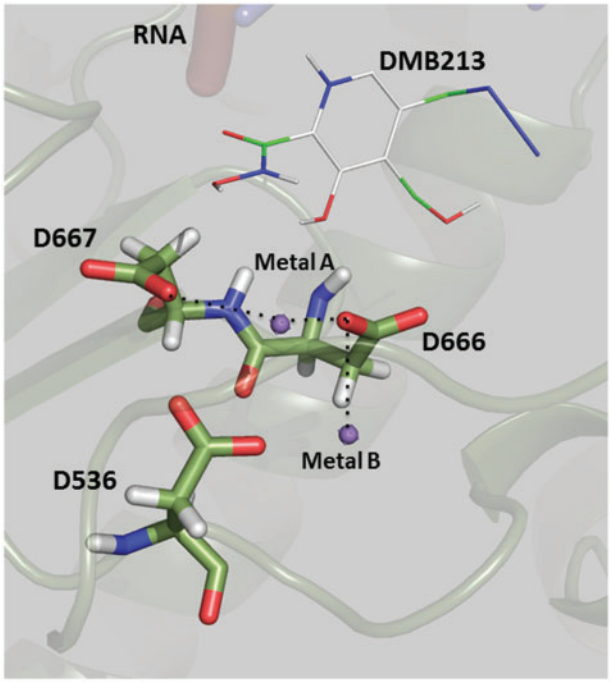

Figure 3. Docking of DMB213 into the active site of the Zika polymerase homology model. DMB213 docks in close proximity to the active site residues D536, D666 and D667. The active site is shown as surface coloured by standard CPK coloration. Blue represents surface-exposed nitrogen and red represents surface-exposed oxygen groups. The proximal location of Mg^{2+} was superimposed into the homology model from the dengue polymerase structure (2J7U) by structure overlay. A short double-stranded RNA was retrieved from the PDB structure 4WTA and overlaid on the homology model structure. Structure visualization was performed using PyMOL. This figure appears in colour in the online version of *JAC* and in black and white in the print version of *JAC*.

Inhibitory effect of sofosbuvir triphosphate on ZIKV RdRp activity in a de novo RdRp assay

To determine the inhibitory effect of sofosbuvir triphosphate on ZIKV NS5 polymerase activity, we used purified recombinant ZIKV NS5 polymerase and heteropolymeric ZMG RNA substrate in a *de novo* ZIKV RdRp assay. We observed that sofosbuvir triphosphate was potent against NS5 polymerase activity, with an IC_{50} of 7.3 μM (Table 1). We also observed an enhanced IC_{50} value (36 μM) for the S604T-mutated RdRp, suggesting that this substitution conferred ∼5-fold resistance to sofosbuvir triphosphate relative to WT enzyme. We also showed that 3′-dGTP inhibited RdRp activity of WT and S604T mutant enzymes with similar potency, with IC_{50}s of ∼0.7 and 0.8 μM, respectively.

Inhibition of ZIKV polymerase activity by the non-nucleoside DMB213 in a primer-dependent RdRp assay

We used homopolymeric poly rC/rG_{13} RNA substrate in an *in vitro* filter-binding ZIKV RdRp assay to screen a large number of pyridoxine-derived compounds for antiviral activity. While most of these were not active in our analysis, one of them, DMB213, was potent against NS5 polymerase activity with IC_{50} of 5.2 μM (Table 2). We also observed a similar IC_{50} value (4.2 μM) for the S604T-mutated RdRp, suggesting that this variant remained susceptible to DMB213 and that sofosbuvir triphosphate and DMB213 possessed different mechanisms of action. The S604T mutant was chosen for this study based on the fact that this residue is highly conserved within the RdRp B motif and was previously shown to confer resistance in HCV to nucleoside analogue inhibitors. As an internal control for the filter-binding RdRp assay, we measured the inhibitory effect of a nucleoside chain terminator 3′-dGTP on ZIKV NS5 polymerase. We showed that 3′-dGTP inhibited RdRp activities of both WT and the S604T mutant enzymes with similar potencies, with IC_{50}s of ∼0.9 μM (Table 2).

Antiviral activity of sofosbuvir and DMB213 against ZIKV in a cell-based assay

To establish the anti-ZIKV activity and relative toxicities of sofosbuvir and DMB213 in cell culture, we used the Promega Viral ToxGlo Assay and Huh7 cells. ZIKV-infected cells were treated with increasing concentrations of sofosbuvir, DMB213 or mycophenolic acid and protection from cytopathic effect was measured. The broad-spectrum antiviral agent mycophenolic acid was used as a positive control of inhibition of ZIKV replication. Experiments were run in duplicate and the data of three independent experiments are summarized in Table 3. The data show that both sofosbuvir and DMB213 were able to inhibit ZIKV, with 50% effective concentrations (EC_{50}s) of 8.3 and 4.6 μM, respectively (Table 3), whereas the EC_{50} for ZIKV of mycophenolic acid was 0.8 μM, in agreement with a recent report.[62] The 50% cytotoxic concentration (CC_{50}) of DMB213 was 22 μM as assayed in Huh7 cells using the Viral ToxGlo Assay (Table 3). Thus, the selectivity index (SI) of DMB213 was below that of sofosbuvir and mycophenolic acid. Accordingly, DMB213 is probably more toxic than sofosbuvir and mycophenolic acid.

Effect of NTP concentration on inhibitory potential of DMB213 against ZIKV NS5 polymerase activity

DMB213 was designed to be able to chelate divalent metal ions from the active site of ZIKV RdRp; therefore, its binding to the RdRp active site might be competitive with that of natural NTP substrates. Previously, we demonstrated that a compound of this same class, i.e. DMB220, was competitive relative to NTPs.[40] To assess this in primer-dependent RdRp reactions with homopolymeric RNA T/P substrate, we used a variety of GTP concentrations in the presence of increasing concentrations of DMB213. We found that the IC_{50} of DMP213 increased as higher concentrations of the GTP substrate were used, which confirms a competitive mechanism of action for DMB213, in agreement with our previous data on DMB220 and DENV (Table 4).

Inhibitory effects of DMB213 on HIV-1 integrase and RT

To test for specificity, we determined whether DMB213 can inhibit the HIV-1 integrase and RT enzymes, which also require metal ion cofactors at the active sites for catalysis. We observed that DMB213 did not inhibit HIV-1 RT activity at concentrations as high as 100 μM (data not shown). In the integrase strand-transfer assay, DMB213 showed a weak inhibitory effect, with an IC_{50} of 13.3 μM in comparison with the IC_{50}s of the approved HIV

integrase inhibitors raltegravir, elvitegravir and dolutegravir, which ranged between 1.6 and 6.8 nM (not shown). Thus, DMB213 possesses apparent specificity for the ZIKV NS5 polymerase.

Molecular docking

Due to the high sequence homology between the Zika and dengue polymerase enzymes, i.e. ∼67% amino acid identity, we used the dengue polymerase structure as a template to generate a homology model of Zika polymerase. The RMSD (root mean square deviation) calculated using PyMOL between the homology model of Zika polymerase obtained from AutoDock Vina and the published structure of dengue polymerase was 0.331 Å.

Alignment of the active site of the dengue polymerase structure (2J7U) and Zika polymerase model shows that the catalytic domain and catalytic residues of dengue polymerase show good superimposition with those of Zika polymerase, suggesting that the position of Mg2+ is appropriate (Figure 3). The Mg2+ ion is close to the expected catalytic position where it is coordinated with residues D536, D666, and D667. DMB213 is also within interaction distance of residues in the catalytic domain (A535, D694, P700 and T702) (not shown). Our docking results are consistent with the observation that DMB213 is a competitive inhibitor of Zika polymerase.

Discussion

This is the first manuscript to report that the NS5 polymerase enzyme of ZIKV can be purified and expressed in *E. coli*. In addition, we have characterized this enzyme in a number of important ways. First, we have demonstrated that RdRp of Zika displays important cation dependency. Second, we have shown that both NIs and NNIs can be active against Zika replication and RdRp activity. Third, we have documented that this enzyme can display drug resistance based on a mutation at position S604T. This is important as this substitution is equivalent in its placement within ZIKV RNA to that of similar substitutions within the polymerase enzymes of HCV and DENV that are also associated with resistance to antiviral compounds.

There is clearly a compelling need to deal with the devastation that has been caused by epidemics attributable to ZIKV. There is widespread consensus that the best hope for a long-term solution is through the development of a safe and effective vaccine that will prevent infection by Zika in the first place. However, in advance of the development and approval of such a vaccine, a compelling case can be made for the use of antiviral drugs. First, the treatment of Zika and the prevention of Zika spread might be attained, in part at least, through the use of antiviral drugs to prevent Zika replication within infected individuals. A case can be made for the treatment of both men and women in order to prevent onward spread and transmission of Zika to the *A. aegypti* mosquito vector.

Although novel drugs need to be investigated in clinical trials prior to approval, hope is provided by the fact that some drugs that have already been approved for other conditions, such as HCV, might also have some anti-Zika activity, as shown here for sofosbuvir. Although the IC_{50} of sofosbuvir is probably higher than desirable in regard to the potential use of this agent to combat Zika, our results provide hope that modifications of sofosbuvir may yield compounds that would be far more effective than sofosbuvir itself. In addition, the use of DMB213, while not ideal because of cell toxicity, also provides hope that novel structures, perhaps based on DMB213, might be generated and be able to play a useful role in regard to anti-Zika drug development.

A major finding of this study is the expression and characterization of the Zika RdRp enzyme itself. We are hopeful that this will lead in short order to the crystallization of this enzyme, which may provide further insights into Zika drug development. At the same time, our work has shown that a mutation at position S604T within the RdRp of Zika can confer resistance to sofosbuvir. Moreover, this work has been confirmed in cell-free RdRp assays. This provides testimony to the importance of this mutation across a wide array of RdRp enzymes that are associated with the *Flaviviridae* family of viruses. Notably, this position seems to be of crucial importance in regard to each of Zika, dengue and HCV.

The work described here is also the first to describe the existence of compounds that might antagonize the replication of ZIKV. Hopefully, this research will shortly kindle new efforts that will lead to the identification of compounds that possess definitive anti-Zika activity and that will be safe and efficacious for human use.

Acknowledgements

We thank Drs David Safronetz and Gary Kobinger for providing ZIKV and Vero E6 cells and Dr Hanh T. Pham and Thibault Mesplède for reviewing the manuscript and assessing results prior to submission. We also thank Mr Cesar Collazos and all other members of the McGill University AIDS Center for providing technical assistance and cooperation.

Funding

This work was partly supported by research grant CCM104886 from the Canadian Institutes of Health Research (CIHR).

Transparency declarations

B. R. S. is an employee of Champlain Exploration Pharma Inc. All other authors: none to declare.

References

1 Westaway EG, Brinton MA, Gaidamovich S *et al*. Flaviviridae. *Intervirology* 1985; **24**: 183–92.

2 Harris E, Holden KL, Edgil D *et al*. Molecular biology of flaviviruses. *Novartis Found Symp* 2006; **277**: 23–39.

3 Dick GW, Kitchen SF, Haddow AJ. Zika virus. I. Isolations and serological specificity. *Trans R Soc Trop Med Hyg* 1952; **46**: 509–20.

4 Tognarelli J, Ulloa S, Villagra E *et al*. A report on the outbreak of Zika virus on Easter Island, South Pacific, 2014. *Arch Virol* 2016; **161**: 665–8.

5 Duffy MR, Chen TH, Hancock WT *et al*. Zika virus outbreak on Yap Island, Federated States of Micronesia. *N Engl J Med* 2009; **360**: 2536–43.

6 Ramos da Silva S, Gao SJ. Zika virus: an update on epidemiology, pathology, molecular biology and animal model. *J Med Virol* 2016; **88**: 1291–6.

7 Weaver SC, Costa F, Garcia-Blanco MA *et al*. Zika virus: history, emergence, biology, and prospects for control. *Antiviral Res* 2016; **130**: 69–80.

8 Fauci AS, Morens DM. Zika virus in the Americas—yet another arbovirus threat. *N Engl J Med* 2016; **374**: 601–4.

9 Brasil P, Sequeira PC, Freitas AD *et al*. Guillain-Barre syndrome associated with Zika virus infection. *Lancet* 2016; **387**: 1482.

10 Rossi SL, Tesh RB, Azar SR *et al*. Characterization of a novel murine model to study Zika virus. *Am J Trop Med Hyg* 2016; **94**: 1362–9.

11 Paixao ES, Barreto F, Teixeira Mda G *et al*. History, epidemiology, and clinical manifestations of Zika: a systematic review. *Am J Public Health* 2016; **106**: 606–12.

12 Tang H, Hammack C, Ogden SC *et al*. Zika virus infects human cortical neural progenitors and attenuates their growth. *Cell Stem Cell* 2016; **18**: 587–90.

13 Li C, Xu D, Ye Q *et al*. Zika virus disrupts neural progenitor development and leads to microcephaly in mice. *Cell Stem Cell* 2016; **19**: 120–6.

14 White MK, Wollebo HS, Beckham JD *et al*. Zika virus: an emergent neuropathological agent. *Ann Neurol* 2016; **80**: 479–89.

15 Sirohi D, Chen Z, Sun L *et al*. The 3.8 A resolution cryo-EM structure of Zika virus. *Science* 2016; **352**: 467–70.

16 Kostyuchenko VA, Lim EX, Zhang S *et al*. Structure of the thermally stable Zika virus. *Nature* 2016; **533**: 425–8.

17 Ladner JT, Wiley MR, Prieto K *et al*. Complete genome sequences of five Zika virus isolates. *Genome Announc* 2016; **4**: e00377-16.

18 van Hemert F, Berkhout B. Nucleotide composition of the Zika virus RNA genome and its codon usage. *Virol J* 2016; **13**: 95.

19 Kuno G, Chang GJ. Full-length sequencing and genomic characterization of Bagaza, Kedougou, and Zika viruses. *Arch Virol* 2007; **152**: 687–96.

20 Zopf S, Kremer AE, Neurath MF *et al*. Advances in hepatitis C therapy: what is the current state - what come's next? *World J Hepatol* 2016; **8**: 139–47.

21 Powdrill MH, Bernatchez JA, Gotte M. Inhibitors of the hepatitis C virus RNA-dependent RNA polymerase NS5B. *Viruses* 2010; **2**: 2169–95.

22 McConachie SM, Wilhelm SM, Kale-Pradhan PB. New direct-acting antivirals in hepatitis C therapy: a review of sofosbuvir, ledipasvir, daclatasvir, simeprevir, paritaprevir, ombitasvir and dasabuvir. *Expert Rev Clin Pharmacol* 2016; **9**: 287–302.

23 Zhao Y, Soh TS, Zheng J *et al*. A crystal structure of the dengue virus NS5 protein reveals a novel inter-domain interface essential for protein flexibility and virus replication. *PLoS Pathog* 2015; **11**: e1004682.

24 Lim SP, Koh JH, Seh CC *et al*. A crystal structure of the dengue virus non-structural protein 5 (NS5) polymerase delineates interdomain amino acid residues that enhance its thermostability and de novo initiation activities. *J Biol Chem* 2013; **288**: 31105–14.

25 Yap TL, Xu T, Chen YL *et al*. Crystal structure of the dengue virus RNA-dependent RNA polymerase catalytic domain at 1.85-angstrom resolution. *J Virol* 2007; **81**: 4753–65.

26 Klema VJ, Ye M, Hindupur A *et al*. Dengue virus nonstructural protein 5 (NS5) assembles into a dimer with a unique methyltransferase and polymerase interface. *PLoS Pathog* 2016; **12**: e1005451.

27 Malet H, Egloff MP, Selisko B *et al*. Crystal structure of the RNA polymerase domain of the West Nile virus non-structural protein 5. *J Biol Chem* 2007; **282**: 10678–89.

28 Lu G, Gong P. Crystal structure of the full-length Japanese encephalitis virus NS5 reveals a conserved methyltransferase-polymerase interface. *PLoS Pathog* 2013; **9**: e1003549.

29 Steitz TA, Steitz JA. A general two-metal-ion mechanism for catalytic RNA. *Proc Natl Acad Sci USA* 1993; **90**: 6498–502.

30 Latour DR, Jekle A, Javanbakht H *et al*. Biochemical characterization of the inhibition of the dengue virus RNA polymerase by β-D-2′-ethynyl-7-deaza-adenosine triphosphate. *Antiviral Res* 2010; **87**: 213–22.

31 Yin Z, Chen YL, Schul W *et al*. An adenosine nucleoside inhibitor of dengue virus. *Proc Natl Acad Sci USA* 2009; **106**: 20435–9.

32 Gotte M, Feld JJ. Direct-acting antiviral agents for hepatitis C: structural and mechanistic insights. *Nat Rev Gastroenterol Hepatol* 2016; **13**: 338–51.

33 Lim SP, Noble CG, Shi PY. The dengue virus NS5 protein as a target for drug discovery. *Antiviral Res* 2015; **119**: 57–67.

34 Malet H, Masse N, Selisko B *et al*. The flavivirus polymerase as a target for drug discovery. *Antiviral Res* 2008; **80**: 23–35.

35 Lim SP, Wang QY, Noble CG *et al*. Ten years of dengue drug discovery: progress and prospects. *Antiviral Res* 2013; **100**: 500–19.

36 Eyer L, Valdes JJ, Gil VA *et al*. Nucleoside inhibitors of tick-borne encephalitis virus. *Antimicrob Agents Chemother* 2015; **59**: 5483–93.

37 Chen H, Liu L, Jones SA *et al*. Selective inhibition of the West Nile virus methyltransferase by nucleoside analogs. *Antiviral Res* 2013; **97**: 232–9.

38 Julander JG, Jha AK, Choi JA *et al*. Efficacy of 2'-C-methylcytidine against yellow fever virus in cell culture and in a hamster model. *Antiviral Res* 2010; **86**: 261–7.

39 Ng KK, Arnold JJ, Cameron CE. Structure-function relationships among RNA-dependent RNA polymerases. *Curr Top Microbiol Immunol* 2008; **320**: 137–56.

40 Xu HT, Colby-Germinario SP, Hassounah S *et al*. Identification of a pyridoxine-derived small-molecule inhibitor targeting dengue virus RNA-dependent RNA polymerase. *Antimicrob Agents Chemother* 2015; **60**: 600–8.

41 Migliaccio G, Tomassini JE, Carroll SS *et al*. Characterization of resistance to non-obligate chain-terminating ribonucleoside analogs that inhibit hepatitis C virus replication in vitro. *J Biol Chem* 2003; **278**: 49164–70.

42 Dutartre H, Bussetta C, Boretto J *et al*. General catalytic deficiency of hepatitis C virus RNA polymerase with an S282T mutation and mutually exclusive resistance towards 2'-modified nucleotide analogues. *Antimicrob Agents Chemother* 2006; **50**: 4161–9.

43 Selisko B, Dutartre H, Guillemot JC *et al*. Comparative mechanistic studies of de novo RNA synthesis by flavivirus RNA-dependent RNA polymerases. *Virology* 2006; **351**: 145–58.

44 Stranix B, Beaulieu F, Bouchard J-E *et al*. *HIV integrase inhibitors from pyridoxine*. US patent US8742123 B2.2009. http://www.google.com/patents/US8742123.

45 Cunha MS, Esposito DL, Rocco IM *et al*. First complete genome sequence of Zika virus (*Flaviviridae*, *Flavivirus*) from an autochthonous transmission in Brazil. *Genome Announc* 2016; **4**: e00032-16.

46 Gong EY, Kenens H, Ivens T *et al*. Expression and purification of dengue virus NS5 polymerase and development of a high-throughput enzymatic assay for screening inhibitors of dengue polymerase. *Methods Mol Biol* 2013; **1030**: 237–47.

47 Ackermann M, Padmanabhan R. De novo synthesis of RNA by the dengue virus RNA-dependent RNA polymerase exhibits temperature dependence at the initiation but not elongation phase. *J Biol Chem* 2001; **276**: 39926–37.

48 Steffens S, Thiel HJ, Behrens SE. The RNA-dependent RNA polymerases of different members of the family Flaviviridae exhibit similar properties in vitro. *J Gen Virol* 1999; **80**: 2583–90.

49 Xu HT, Martinez-Cajas JL, Ntemgwa ML *et al*. Effects of the K65R and K65R/M184V reverse transcriptase mutations in subtype C HIV on enzyme function and drug resistance. *Retrovirology* 2009; **6**: 14.

50 Xu HT, Asahchop EL, Oliveira M *et al*. Compensation by the E138K mutation in HIV-1 reverse transcriptase for deficits in viral replication capacity and enzyme processivity associated with the M184I/V mutations. *J Virol* 2011; **85**: 11300–8.

51 Xu HT, Colby-Germinario SP, Quashie PK *et al*. Subtype-specific analysis of the K65R substitution in HIV-1 that confers hypersusceptibility to a novel nucleotide-competing reverse transcriptase inhibitor. *Antimicrob Agents Chemother* 2015; **59**: 3189–96.

52 Bar-Magen T, Donahue DA, McDonough EI *et al*. HIV-1 subtype B and C integrase enzymes exhibit differential patterns of resistance to integrase inhibitors in biochemical assays. *AIDS* 2010; **24**: 2171–9.

53 Quashie PK, Mesplede T, Han YS *et al*. Characterization of the R263K mutation in HIV-1 integrase that confers low-level resistance to the second-generation integrase strand transfer inhibitor dolutegravir. *J Virol* 2012; **86**: 2696–705.

54 Zhang Y. I-TASSER server for protein 3D structure prediction. *BMC Bioinformatics* 2008; **9**: 40.

55 Roy A, Kucukural A, Zhang Y. I-TASSER: a unified platform for automated protein structure and function prediction. *Nat Protoc* 2010; **5**: 725–38.

56 Yang J, Roy A, Zhang Y. Protein-ligand binding site recognition using complementary binding-specific substructure comparison and sequence profile alignment. *Bioinformatics* 2013; **29**: 2588–95.

57 Appleby TC, Perry JK, Murakami E *et al*. Viral replication. Structural basis for RNA replication by the hepatitis C virus polymerase. *Science* 2015; **347**: 771–5.

58 Pettersen EF, Goddard TD, Huang CC *et al*. UCSF Chimera – a visualization system for exploratory research and analysis. *J Comput Chem* 2004; **25**: 1605–12.

59 Trott O, Olson AJ. AutoDock Vina: improving the speed and accuracy of docking with a new scoring function, efficient optimization, and multithreading. *J Comput Chem* 2010; **31**: 455–61.

60 Sheik SS, Sundararajan P, Hussain AS *et al*. Ramachandran plot on the web. *Bioinformatics* 2002; **18**: 1548–9.

61 Kolaskar AS, Sawant S. Prediction of conformational states of amino acids using a Ramachandran plot. *Int J Pept Protein Res* 1996; **47**: 110–6.

62 Barrows NJ, Campos RK, Powell ST *et al*. A screen of FDA-approved drugs for inhibitors of Zika virus infection. *Cell Host Microbe* 2016; **20**: 259–70.